Structural Behavior Of Thermoplastic Welded Single-lap Shear Joints With Recycled Core Material

Schiller, A.; Bisagni, C.

Publication date
2024

Document Version
Final published version

Published in
Proceedings of the 21st European Conference on Composite Materials

STRUCTURAL BEHAVIOR OF THERMOPLASTIC WELDED SINGLE-LAP SHEAR JOINTS WITH RECYCLED CORE MATERIAL

A. Schiller[1] and C. Bisagni[2]

[1]Faculty of Aerospace Engineering, Delft University of Technology, 2629 HS Delft, Netherlands
Email: A.Schiller@tudelft.nl
[2]Faculty of Aerospace Engineering, Delft University of Technology, 2629 HS Delft, Netherlands
Email: C.Bisagni@tudelft.nl

Keywords: Recycling, Single-Lap Shear Joint, Thermoplastic Welding, Damage Growth

Abstract

Composite single-lap shear joints made from virgin plies and recycled core material are manufactured via induction and conduction welding using T300/polyphenylene sulfide (T300/PPS) as well as T700/low-melt polyaryletherketone (T700/LM-PAEK). The specimens are tested in quasi-static conditions to evaluate their mechanical performance and damage growth. Digital image correlation and high-speed cameras are used to capture the specimen behavior until after failure. While joints with recycled core material show a lower load-transferring capacity than their virgin counterparts (reduction of 13.8% for T300/PPS and 41.2% for T700/LM-PAEK), they are nonetheless an appealing option for applications where sustainability is a priority. Damage in virgin thermoplastic welded single-lap shear joints grows along the weld line. Conversely, specimens containing recycled core material may also experience delaminations between the core and the virgin outer plies. This suggests that thermoplastic welding can create interfaces with higher fracture toughness properties than those achieved during the consolidation of the base laminates.

1. Introduction

One of the great challenges of our time is the realignment of society and industry towards more sustainability. The European Union has set the ambitious goal to make Europe the first climate neutral continent by 2050 [1]. Consequently, the transportation sector and especially the aerospace industry are required to significantly reduce their impact on the environment. One way to design more environmentally friendly aircraft is to utilize materials with more advantageous properties, for example thermoplastic composites. These materials feature similar strength-to-weight ratios as their thermosetting counterparts, but also provide the opportunity for recycling, high toughness, and may be manufactured cost-efficiently as well as in high volumes using thermoplastic welding [2]. While many studies have been published on the effects of either recycling or of welding on the mechanical response of thermoplastic structures [3,4], their interaction is not yet well understood.

The recycling of carbon fiber-reinforced polymers (CFRPs) can be classified into mechanical, thermal, and chemical methods. Both thermal and chemical recycling aim at separating the matrix material from the carbon fibers. Milling, a mechanical approach, works by reducing larger pieces of CFRP to fine powder or short fiber recyclate and is generally considered to be one of the most mature technologies for the recycling of fiber-reinforced polymers [5].

Several techniques for thermoplastic welding have been developed, for example induction welding, resistance welding, and ultrasonic welding [6]. Conduction welding is a more recent addition to this group, but has found interest because of its scaling potential for manufacturing [7]. Neither induction nor conduction welding require the use of energy directors in the weld line which reduces the complexity of the joining process [8].

The aim of this paper is to investigate the influence of recycled (milled) thermoplastic CFRP on the structural performance of induction and conduction welded single-lap shear joints. Therefore, an experimental test campaign was conducted to compare the mechanical response of these structures. In addition, damage initiation and propagation in the joints were studied to relate the joint constituents to the observed failure modes.

2. Welded Single-Lap Shear Specimens

Virgin fabric Toray Cetex® TC1100 PPS [9], which consists of T300 carbon fibers in a polyphenylene sulfide (PPS) matrix, and virgin unidirectional (UD) Toray Cetex ®TC1225 LMPAEK™ [10], which is made from T700 fibers embedded in low-melt polyaryletherketone (LM-PAEK), are consolidated to composite laminates at Collins Dutch Thermoplastic Components (DTC). Due to the nature of the raw materials (fabric and UD plies), two distinct layups are considered: [(±45),(0/90),(±45),(0/90),(±45),(0/90),(±45)] for T300/PPS and $[45/90/-45/0]_{2S}$ for T700/LM-PAEK with nominal thicknesses of 2.4 mm and 2.2 mm, respectively. Scrap material from each production cycle is collected and milled to a fine shred with chip sizes of less than 5 mm. The recycled material is placed between two 0° face sheets of the corresponding virgin fiber-reinforced polymer and reconsolidated. Single-lap shear joints are subsequently manufactured from the four different laminates using induction welding at the Dutch Aerospace Center (Nederlands Lucht- en Ruimtevaartcentrum, NLR) and employing conduction welding at Collins DTC. A summary of the different specimens is given in Table 1.

Table 1. Overview of specimen materials and joining methods.

ID	No.	Material Type	Constituents	Welding Technique	Welding Temperature
A	5	Virgin	T300/PPS	Induction	364°C
B	5	Virgin & Recycled Core	T300/PPS	Induction	365°C
C	5	Virgin	T700/LM-PAEK	Conduction	385°C
D	13	Virgin & Recycled Core	T700/LM-PAEK	Conduction	385°C

The specimen geometry follows the ASTM standard D5868 [11] and is sketched in Figure 1. Nominal and average dimensions per specimen type are summarized in Table 2.

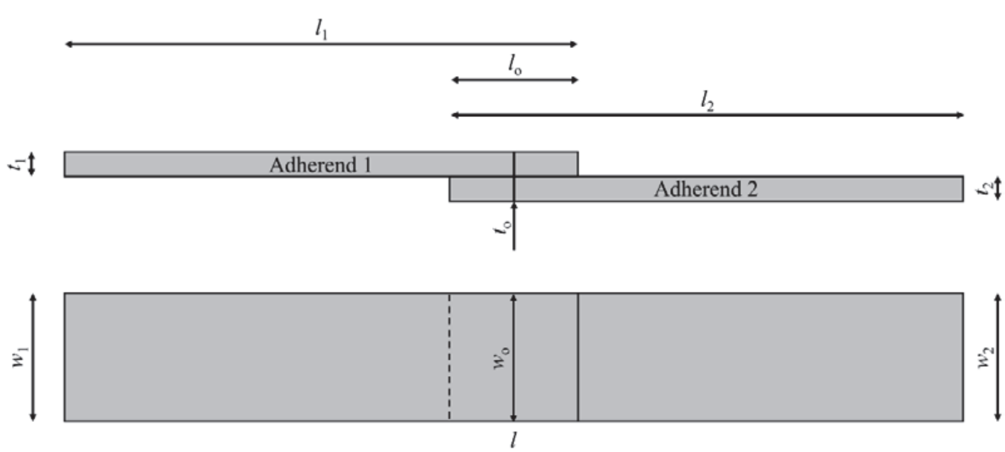

Figure 1. Specimen geometry.

Table 2. Nominal and average specimen dimensions.

	Symbol	Unit	Nominal	A	B	C	D
Total Length	l	mm	177.8	177.5	177.9	171.0	177.3
Length Adherend 1	l_1	mm	101.6	101.7	101.7	101.6	102.3
Width Adherend 1	w_1	mm	25.4	25.4	25.4	25.4	24.2
Thickness Adherend 1	t_1	mm	2.4/2.2	2.4	2.5	2.3	3.6
Length Adherend 2	l_2	mm	101.6	101.7	101.7	101.7	104.3
Width Adherend 2	w_2	mm	25.4	25.4	25.4	25.4	24.0
Thickness Adherend 2	t_2	mm	2.4/2.2	2.4	2.4	2.3	3.6
Width Overlap	w_o	mm	25.4	25.4	25.5	25.5	24.1
Thickness Overlap	t_o	mm	4.8/4.4	5.0	5.1	4.5	6.5
Length Overlap	l_o	mm	25.4	25.9	25.5	32.4	29.3

Images of the specimens from each of the four sets are shown in Figure 2 after they have been painted white and a black speckle pattern for digital image correlation (DIC) has been applied. Additionally, vertical lines are marked on one side of the overlap region to measure the crack length in this area.

(a)

(b)

(c)

(d)

Figure 2. Specimens made from (a) virgin T300/PPS, (b) T300/PPS with recycled core material, (c) virgin T700/LM-PAEK, and (d) T700/LM-PAEK with recycled core material.

3. Test Procedure

The single-lap shear joints are loaded in displacement-control at a speed of 0.2 mm/min (virgin T300/PPS specimens) and 0.1 mm/min (all other samples) in a Zwick-Roell Universal Test Machine with adjustable grips using a 250 kN load cell. Machine displacement is measured with a linear variable differential transformer (LVDT).

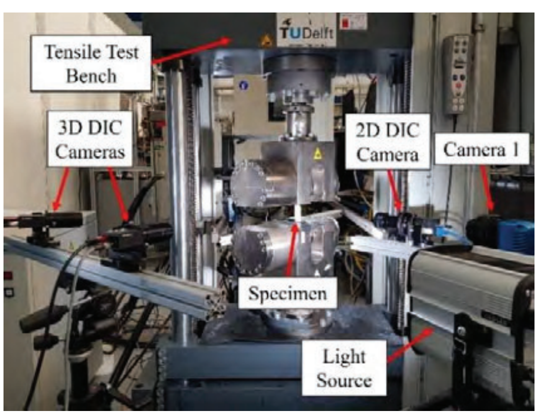

(a)

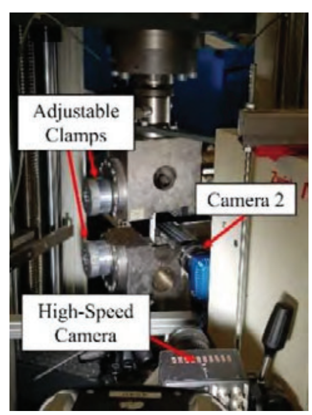

(b)

Figure 3. Single-lap shear test setup: (a) front and (b) rear view.

Two 3D DIC cameras measure the displacement on the front of the specimens, and one 2D DIC camera tracks the deformation on the right side of the overlap region. Then, two additional cameras are used: Camera 1 takes isometric pictures of the single-lap shear joints during the tests while Camera 2 captures the crack initiation and propagation on the left side of the overlap area. In addition, a high-speed camera records the final fracture of the joint.

Load-displacement data is recorded after a preload of 50 N has been applied to the specimen. This offset is corrected by running a linear least squares analysis that calculates the initial stiffness of the joint. The initial joint stiffness is then used to compute the expected displacement at the preload. Adding the preload displacement to the LVDT displacement from the test machine yields the corrected displacement data which is used in the load-displacement curves for all further evaluations.

Damage in single-lap shear joints typically initiates in the form of cracks at the overlap ends. Cracks cause large local deformations and therefore significant strains. These displacements and strains can be captured with DIC. Here, 2D DIC on the right side of the overlap region is used. The 2D DIC images are post-processed with the Vic-2D 6 software distributed by Correlated Solutions. Determining a threshold strain value at the crack tip in one DIC image allows applying a simple strain-based failure criterion to track the damage propagation in a specimen over the remaining DIC images.

4. Joint Performance: Virgin vs. Recycled Core

The average maximum load, average lap shear strength, and average initial joint stiffness of the four specimen sets are evaluated to investigate how the recycled core material influences the mechanical performance of the single-lap shear joints. An overview of these three quantities is given in Table 3. Two T700/LM-PAEK recycled core joints failed in the adherend cross-section close to the clamps. Hence, they were excluded from the calculation of the average mechanical performance of the corresponding specimen set.

Table 3. Average maximum load, lap shear strength, and initial joint stiffness (±standard deviation).

ID	Specimen Type	Maximum Load [kN]	Shear Strength [MPa]	Initial Stiffness [kN/mm]
A	T300/PPS	13.42 ± 0.31	20.40 ± 0.50	12.91 ± 0.25
B	T300/PPS (Recycled Core)	11.39 ± 0.68	17.58 ± 1.04	9.98 ± 0.60
C	T700/LM-PAEK	10.98 ± 1.58	13.32 ± 1.84	12.52 ± 0.14
D	T700/LM-PAEK (Recycled Core)	5.56 ± 0.90	7.83 ± 1.22	11.80 ± 0.99

Since the dimensions of specimen sets A and B (virgin and recycled core induction welded fabric T300/PPS) are almost identical, the variation in the mechanical response between the two sets can be directly correlated to the change in material properties due to the different materials. The maximum load of the joints reduces by 15.1% from 13.42 kN (virgin) to 11.39 kN (recycled core). Similarly, the apparent shear strength decreases by 13.8% (20.4 MPa to 17.58 MPa) while the initial joint stiffness at the beginning of the test drops from 12.91 kN/mm to 9.98 kN/mm which amounts to a reduction of 22.7%. Meanwhile, the standard deviation of all three metrics more than doubles.

The average maximum load and shear strength of the various specimen sets do not necessarily decrease by the same percentage because of the slightly different overlap areas considered for calculating the lap shear strength (Table 2). The increase in the standard deviation of the test results is a direct consequence of the use of the recycled core material. The shredded fibers are neither evenly distributed nor uniformly oriented in the adherends and therefore give rise to a locally varying material stiffness which causes stress concentrations. If unfavorable material distributions coincide with regions that are highly loaded i.e., the overlap ends of single-lap shear joints, then a significant decrease in strength may be the result compared to the virgin material. Furthermore, short fibers cannot transfer as high loads as continuous fibers which explains the reduction in joint stiffness.

CONTENTS

These trends are also visualized in Figure 4a where load-displacement curves for the T300/PPS specimens are plotted. While the curves for virgin joints are closely spaced, both a considerable decrease in joint stiffness as well as a wider spread of test results are apparent for recycled core samples.

Likewise, a reduction of the mechanical performance is visible for conduction welded UD T700/LM-PAEK in Figure 4b when comparing virgin and recycled core specimens. While the average maximum load drops by 49.3% from 10.98 kN to 5.56 kN, shear strength and initial joint stiffness decrease by 41.2% (13.32 MPa to 7.83 MPa) and 5.8% (12.52 kN/mm to 11.8 kN/mm), respectively. In contrast to the T300/PPS specimens, the standard deviations of the T700/LM-PAEK test results reduce for both maximum load and shear strength, but not for initial joints stiffness.

The relatively modest drop in stiffness compared to the large reduction in load-carrying capacity can be explained with the increase in adherend thickness (Table 2). The inverted trends for the standard deviation are not caused by unexpected behavior of the recycled core joints, but rather by the large range of test results for virgin T700/LM-PAEK specimens shown in Figure 4b. The maximum loads of the virgin specimens can be correlated to their location during conduction welding which indicates a bias introduced during the joining process.

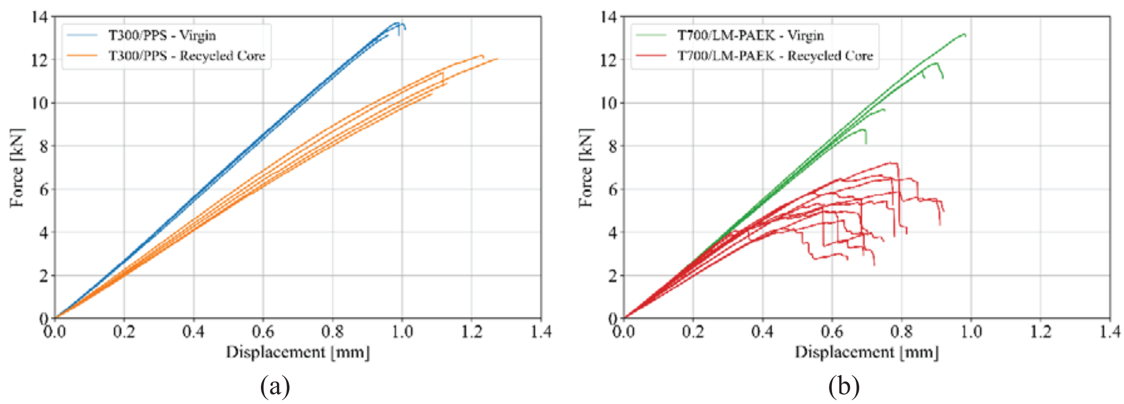

Figure 4. Load-displacement curves for (a) T300/PPS and (b) T700/LM-PAEK single-lap shear joints.

5. Damage Initiation, Propagation, and Failure

Damage in virgin T300/PPS and T700/LM-PAEK single-lap shear joints follows the pattern illustrated in Figure 5. Cracks initiate at relatively low loads at both overlap ends and then grow towards each other along the weld line. Crack growth is stable until the maximum load is reached. Afterwards, it becomes unstable, and the specimen fails. A highly strained weld line can be observed just before fracture at 13.1 kN. The specimen breaks due to shear failure along the weld line.

The relatively low damage initiation loads are attributed to the fact that the specimens are only completely welded in the center of the overlap region. Towards the overlap ends, the interface experiences lower temperatures during welding and therefore the thermoplastic matrix does not fully melt and reconsolidate. As a result, lower fracture toughness values can be expected in these regions which lead to cracks at comparatively small loads.

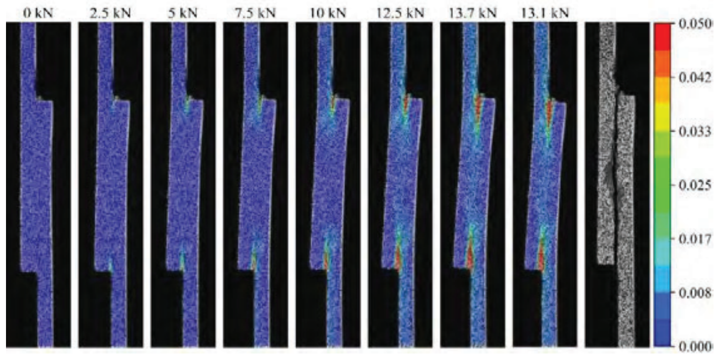

Figure 5. Crack growth in a virgin T300/PPS specimen visualized with 2D DIC using the major principal strain ε_1.

Similarly, damage initiation in the T300/PPS recycled core specimen in Figure 6 can be detected for loads as low as 0.4 kN at the upper overlap end. The same crack has not propagated at 2.5 kN, but has become more visible due to the specimen rotating because of secondary bending. Interestingly, no crack initiation is observed at the lower overlap end. Instead, a delamination between the virgin outer ply and the recycled core material forms at a load of around 7.5 kN. Again, damage propagation is stable for both the crack and the delamination until the maximum load is reached. However, failure does not occur along the weld line in this case. Rather, the delamination growth extends into a transverse crack through the recycled core material and leads to adherend failure at the lower overlap end.

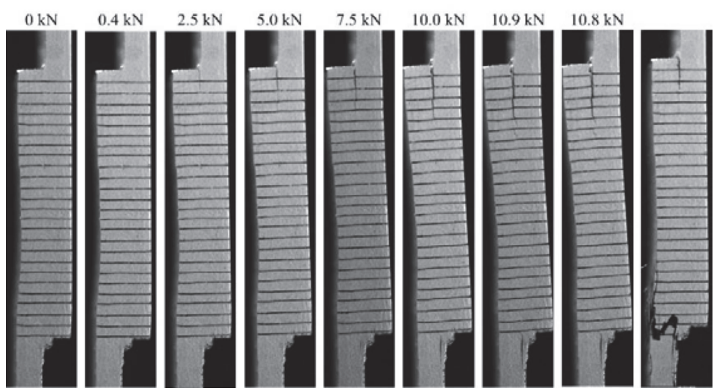

Figure 6. Crack growth in a T300/PPS recycled core specimen.

The change in damage evolution and failure mode is most likely a result of multiple phenomena. First, the small step at the lower overlap end appears to provide a sufficient gradual change in stiffness which delays crack initiation there. Second, since overlap ends are free edges, high interlaminar stresses exist in these regions and may trigger delaminations. This suggests that the fracture toughness properties inside the weld region are higher than those in the adherends between the virgin plies and the recycled core material.

Such a conclusion is supported by Figure 7 which illustrates the failure modes of four different T300/PPS specimens with recycled core material welded at nominally identical temperatures. However, thermocouple data shows that the temperature close to each weld line ranges from 365.4°C in Figure 7a to 379.6°C in Figure 7d. Evidently, the failure mode changes with increasing welding temperature. Figure 7a shows pure shear failure along the weld line. Shear failure along the weld line is also the dominant failure mode in Figure 7b, but a transverse crack is visible at the left (lower) overlap end. In Figure 7c the crack growth from the right (upper) overlap end does not reach the left side and instead adherend failure is observed. The specimen in Figure 7d is the same one as in Figure 6 and exhibits exclusively adherend failure. Hence, the weld interface must become stronger with increasing welding temperature which results in the adherend strength becoming critical. In addition, this implies that the shear strength data in Table 3 for the T300/PPS recycled core specimens is not actually representative of the shear strength of the weld line.

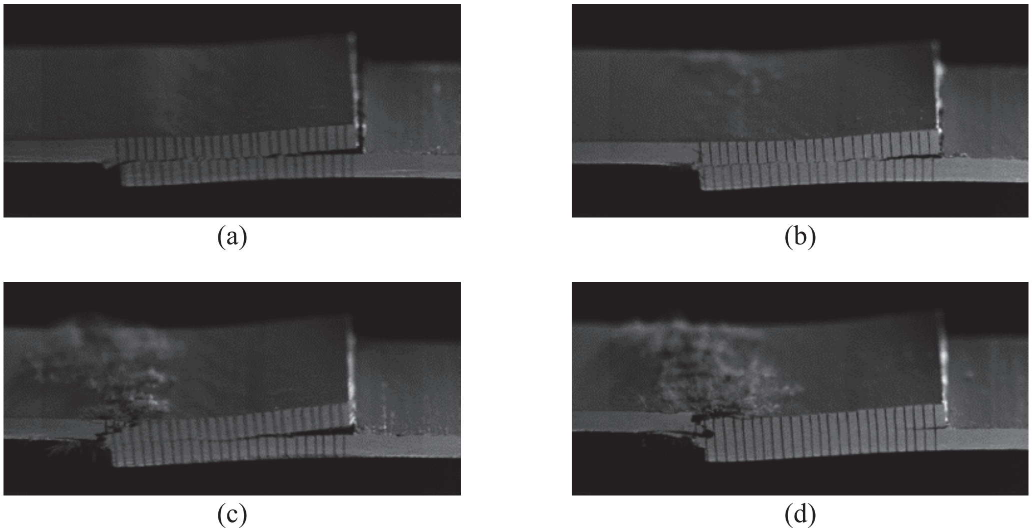

Figure 7. Failure modes of four different recycled core T300/PPS joints captured with a high-speed camera at 50000 frames per second.

Damage in the recycled core T700/LM-PAEK specimens always initiates at the lower overlap end as shown in Figure 8. The high pressure and temperature applied during welding forces some recycled core material to flow out of the overlap region. It then reconsolidates on top of one of the adherends and forms a step that reduces the stress concentration in this region, thus inhibiting damage initiation.

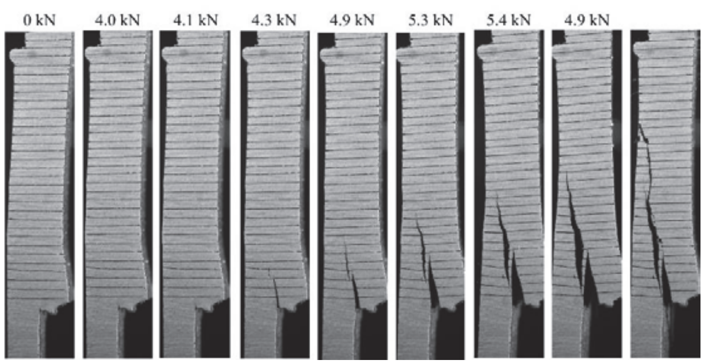

Figure 8. Crack growth in a T700/LM-PAEK recycled core specimen.

The crack at the lower overlap end is eventually accompanied by another delamination between the outer virgin ply and the recycled core material at a load of around 4.3 kN. Since the T700/LM-PAEK joints feature large out-of-plane deformations due to welding (Figures 2c and 2d), the test machine bends the upper adherend around the forming delamination in an attempt to align the adherend with its own axis. Crack growth in all loading phases is stable, and final failure occurs when the strength of the core material is exceeded. Like the recycled core T300/PPS specimens, the lap shear strength of the welded T700/LM-PAEK joints with recycled core material is higher than the strength of the adherends themselves.

6. Conclusions

Thermoplastic welded composite single-lap shear joints made from virgin T300/polyphenylene sulfide (T300/PPS) and T700/low-melt polyaryletherketone (T700/LM-PAEK) as well as recycled core material have been tested in quasi-static conditions to compare their mechanical performance. In addition, damage initiation, propagation, and failure modes of these structures were investigated. While integrating recycled core material into the joints reduced the lap shear strength of the specimens from 20.40 MPa to 17.58 MPa for induction welded T300/PPS and from 13.32 MPa to 7.83 MPa for conduction welded T700/LM-PAEK, the recycled core specimens nevertheless showed potential for applications where some load-carrying capacity can be traded off for a smaller environmental impact.

Damage in thermoplastic welded single-lap shear joints with virgin material initiated with two cracks at the overlap ends and propagated in a stable manner until the maximum load was reached. Failure occurred along the weld line. Damage and failure modes in joints with recycled core material were less consistent and depend on the welding temperature of the specimens. Both cracks at overlap ends and delaminations in the adherends were observed. Joint interfaces welded at high temperatures may feature higher fracture toughness properties than the adherends, thus resulting in adherend fracture instead of shear failure along the weld line.

Acknowledgments

This research was carried out as part of the SUSTAINair project. The authors gratefully acknowledge the financial support received from the European Union's Horizon 2020 research and innovation programme under grant agreement number 101006952. The authors would also like to express their gratitude to Collins DTC and to the NLR for specimen production.

References

[1] *European Green Deal – Delivering on our Targets*. Publications Office of the European Union, Luxembourg, 2021.
[2] B. Tijs, S. Abdel-Monsef, J. Renart, A. Turon and C. Bisagni. Characterization and analysis of the interlaminar behavior of thermoplastic composites considering fiber bridging and R-curve effects. *Composites Part A: Applied Science and Manufacturing*, 162:107101, 2022.
[3] S. Pimenta and S. Pinho. Recycling carbon fibre reinforced polymers for structural applications: Technology review and market outlook. *Waste Management*, 31(2): 378-392, 2011.
[4] C. Ageorges, L. Ye and M. Hou. Advances in fusion bonding techniques for joining thermoplastic matrix composites: A review. *Composites Part A: Applied Science and Manufacturing*, 32: 839-857, 2001.
[5] J. Zhang, V. Chevali, H. Wang and C. Wang. Current status of carbon fibre and carbon fibre composites recycling. *Composites Part B: Engineering*, 193: 108053, 2020.
[6] I. Villegas, L. Moser, A. Yousefpour, P. Mitschang and H. Berse. Process and performance evaluation of ultrasonic, induction, and resistance welding of advanced thermoplastic composites. *Journal of Thermoplastic Composite Materials*, 26(8): 1007-1024, 2013.
[7] B. Tijs, M. Doldersum, A. Turon, J. Waleson and C. Bisagni. Experimental and numerical evaluation of conduction welded thermoplastic composite joints. *Composite Structures*, 281: 114964, 2022.
[8] T. Ahmed, D. Stavrov, H. Berse and A. Beukers. Induction welding of thermoplastic composites – an overview. *Composites Part A: Applied Science and Manufacturing*, 37(10): 1638-1651, 2006.
[9] Toray Advanced Composites. *Toray Cetex® TC1100 PPS Product Data Sheet*. 2021.
[10] Toray Advanced Composites. *Toray Cetex® TC1225 LMPAEK™ Product Data Sheet*. 2023.
[11] ASTM International. *ASTM D5868-01: Standard Test Method for Lap Shear Adhesion for Fiber Reinforced Plastic (FRP) Bonding*. 2023.